PAPER • OPEN ACCESS

Fluctuation theorem between non-equilibrium states in an *RC* circuit

New Journal of Physics
The open access journal at the forefront of physics

Deutsche Physikalische Gesellschaft DPG
IOP Institute of Physics

Published in partnership with: Deutsche Physikalische Gesellschaft and the Institute of Physics

OPEN ACCESS

RECEIVED
2 February 2015

REVISED
20 April 2015

ACCEPTED FOR PUBLICATION
5 May 2015

PUBLISHED
4 June 2015

PAPER

Fluctuation theorem between non-equilibrium states in an *RC* circuit

L Granger[1,2,5], **J Mehlis**[2,3,4], **É Roldán**[2,5], **S Ciliberto**[4] **and H Kantz**[2]

[1] Departamento de Física Atómica, Molecular y Nuclear, Universidad Complutense de Madrid, E-28040 Madrid, Spain
[2] Max-Planck Institut für Physik komplexer Systeme, Nöthnitzer Str. 38, D-01187 Dresden, Germany
[3] Martin-Luther-Universität Halle-Wittenberg, Von-Danckelmann-Platz 3, D-06120 Halle, Germany
[4] Université de Lyon, Laboratoire de Physique, École Normale Supérieure de Lyon, CNRS UMR5672, 46 allée d'Italie, F-69364 Lyon Cedex 07, France
[5] Grupo Interdisciplinar de Sistemas Complejos (GISC), Madrid, Spain

E-mail: leogranger@ucm.es

Keywords: fluctuation theorems, stochastic thermodynamics, entropy production

Abstract

Fluctuation theorems impose constraints on the probability of observing negative entropy production in small systems driven out of equilibrium. The range of validity of fluctuation theorems has been extensively tested for transitions between equilibrium and non-equilibrium stationary states, but not between general non-equilibrium states. Here we report an experimental verification of the detailed fluctuation theorem for the total amount of entropy produced in the isothermal transition between two non-equilibrium states. The experimental setup is a parallel *RC* circuit driven by an alternating current. We investigate the statistics of the heat released, of the variation of the entropy of the system, and of the entropy produced for processes of different durations. We show that the fluctuation theorem is satisfied with high accuracy for current drivings at different frequencies and different amplitudes.

1. Introduction

As already noted by Szilard in 1925 [1], entropy reduction can occur in a single realization of a thermodynamic process at the mesoscopic scale and the second law of thermodynamics is recovered when averaging over many realizations of such a process. At scales where thermal fluctuations are relevant, entropy-reducing trajectories can be observed [2, 3]. The fluctuations of the entropy production are governed by the so-called *fluctuation theorems*, which relate the probability to observe a trajectory destroying a certain amount of entropy to the probability to observe a trajectory producing the same amount of entropy [4–14]. In particular, they ensure that on average, the entropy production is positive. The fluctuation theorems are the building blocks of the emerging theory of stochastic thermodynamics, which describes the equilibrium and non-equilibrium thermodynamics of small systems, at the ensemble level as well as at the trajectory level [10, 15–21]. In parallel to the theoretical development of stochastic thermodynamics, the fluctuation theorems and the thermodynamics of small systems has been intensively investigated experimentally in last decade [2, 3, 22–30].

The fluctuation theorem for the total entropy production relates the probability $P(\Delta S_{\rm tot})$ to observe a trajectory producing an amount $\Delta S_{\rm tot}$ of entropy in a given thermodynamic process to the probability $\tilde{P}(-\Delta S_{\rm tot})$ to observe a trajectory destroying the very same amount of entropy in the time reversed or *backward* process, where the driving of the system is reversed in time [8, 11, 13, 14]:

$$\frac{P(\Delta S_{\rm tot})}{\tilde{P}(-\Delta S_{\rm tot})} = \exp\left(\frac{\Delta S_{\rm tot}}{k_{\rm B}}\right). \tag{1}$$

Equation (1) has a wide range of validity: it is valid for systems in contact with one or many heat baths, for transitions between stationary or non-stationary states or for systems in non-equilibrium stationary states. This fluctuation theorem has been experimentally tested for the transition between equilibrium states [3, 33], where it reduces to Crooks' relation [7], for non-equilibrium steady-states [25, 27], and in the transition between non-equilibrium steady-states [23], where it can be refined to give the Hatano–Sasa relation [9]. More recently, the

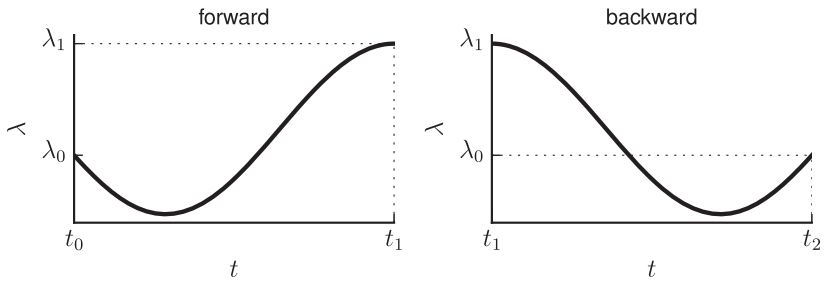

Figure 1. Forward (left panel) and time reverse (right panel) protocols.

fluctuation theorem (1) was observed in a more general experiment involving a periodically driven system in contact with two heat baths at different temperatures [31]. All the aforementioned experiments have this in common, that at the end of the backward process, the system is in the same macroscopic state as at the beginning of the forward process[6].

In this paper, we report an experimental verification of the fluctuation theorem (1) in a situation where this is not case: in our experiment, the final state of the backward process is in general different from the state the system was prepared in at the beginning of the forward process. In such a transition, the fluctuation theorem (1) presents a subtlety, as realized by Spinney and Ford [14]. In fact, in general, the distribution $\tilde{P}$ appearing in the denominator in the left-hand side of equation (1) is not the probability distribution of the entropy produced in the backward process. In general, $\tilde{P}$ is the distribution of a quantity which we will call *conjugated entropy production* in the following. However, in situations were the final state of the backward process is the same as the initial state of the forward process, conjugated entropy production and entropy produced in the backward process are equal. Hence, in those cases, $\tilde{P}$ is the probability distribution of the entropy produced in the backward process.

Our experimental system is a parallel *RC* circuit driven by an alternating current. We verify the fluctuation theorem (1) for processes of arbitrary durations for different driving frequencies and intensities, where we go far beyond the slow driving considered in [30, 31]. Furthermore, we show the difference between conjugated entropy production and entropy produced in the backward process.

The paper is organized as follows. We begin by sketching the derivation of the fluctuation theorem (1) in section 2. In the derivation, we insist on the difference between the conjugated entropy production and entropy produced in the backward process. We continue by describing the experimental setup and protocol in section 3. In particular, we show how we sample forward and backward trajectories making the transition between two non-equilibrium states. Finally, we present our experimental results in section 4. We study the statistics of the heat dissipated to the environment, of the entropy produced and of the conjugated entropy production for different driving times. Furthermore, we show that the fluctuation theorem (1) is satisfied for different driving speeds and amplitudes. We close the paper with a short discussion of our results in section 5.

2. Detailed fluctuation theorem for the transition between two non-equilibrium states

We now sketch the derivation of equation (1) for the transition between two non-equilibrium states. Consider a small system in contact with a heat bath at temperature T, that can be driven by varying a control parameter λ. Initially, the value of the control parameter is set to $\lambda(t_0) = \lambda_0$ and the system is prepared in a non-equilibrium macroscopic state $\rho(q, t_0) = \rho_0(q)$. In other words, at time t_0, the probability that the mesoscopic state of the system is q is given by the non-equilibrium distribution $\rho(q, t_0)$. Due to the presence of thermal fluctuations, the mesoscopic state of the system cannot be controlled, but only the *probability distribution* of mesoscopic states. From time t_0 to t_1, the control parameter is changed from $\lambda(t_0) = \lambda_0$ to $\lambda(t_1) = \lambda_1$ according to a prescribed protocol $\lambda(t)$. The final macroscopic state of the system is $\rho(q, t_1) = \rho_1(q)$. In the backward process, the initial state of the system is the final state of the forward process, $\rho_1(q)$, and the control parameter takes the same values as in the forward case but runs them backwards in time. Hence, we assume that the time reverse process starts just after the forward process ends, at time $t = t_1$. The control parameter is then varied according to $\lambda(t_1 + t) = \lambda(t_1 - t)$, as sketched in figure 1. The backward process ends at time $t_2 = t_1 + \tau$ where $\tau = t_1 - t_0$ is the duration of both the forward and time reverse process. The final macroscopic state of the system is $\rho(q, t_2) = \rho_2(q)$ which is in general different from $\rho_0(q)$.

[6] In fact, in the setup of [31], the macroscopic state is time periodic and the succession of forward and backward processes correspond to one period. The experiments described in [3, 23, 25, 33] involve transitions between (equilibrium or non-equilibrium) stationary states.

The amount of entropy produced by a trajectory $\mathbf{m} = \{q_t\colon\ t_0 \leqslant t \leqslant t_1\}$ in the forward process is given by [13, 34–36]:

$$\Delta S_{\rm tot}[\mathbf{m}] = k_{\rm B} \log \frac{\mathcal{P}_{\rm F}[\mathbf{m}]}{\mathcal{P}_{\rm B}[\tilde{\mathbf{m}}]}, \tag{2}$$

where $\mathcal{P}_{\rm F}[\mathbf{m}]$ is the probability to observe the trajectory $\mathbf{m}$ in the forward process and $\mathcal{P}_{\rm B}[\tilde{\mathbf{m}}]$ is the probability to observe the time reverse trajectory $\tilde{\mathbf{m}}$ of $\mathbf{m}$ in the backward process. The time reverse trajectory $\tilde{\mathbf{m}}$ contains the same states as $\mathbf{m}$, but runs backwards in time: $\tilde{\mathbf{m}}(t_1 + t) = \mathbf{m}(t_1 - t)$ [7]. The definition of entropy production in (2) is consistent with the usual thermodynamic definition [34–36]:

$$\Delta S_{\rm tot}[\mathbf{m}] = \frac{Q[\mathbf{m}]}{T} + \Delta S[\mathbf{m}], \tag{3}$$

where $Q[\mathbf{m}]$ is the amount of heat dissipated to the environment along the trajectory $\mathbf{m}$ and $\Delta S[\mathbf{m}] = -k_{\rm B} \log \rho_1(q_1) + k_{\rm B} \log \rho_0(q_0)$ is the variation of the trajectory dependent entropy of the system along the trajectory $\mathbf{m}$ [10]. In fact, it can be shown that [10, 13, 26, 37]:

$$\frac{Q[\mathbf{m}]}{T} = k_{\rm B} \log \frac{\mathcal{P}_{\rm F}\left[\mathbf{m}\,\middle|q_0\right]}{\mathcal{P}_{\rm B}\left[\tilde{\mathbf{m}}\middle|\,q_1\right]}, \tag{4}$$

where $\mathcal{P}_{\rm F}[\mathbf{m}\,|q_0]$ is the probability to observe the trajectory $\mathbf{m}$ given the initial state q_0, and $\mathcal{P}_{\rm B}[\tilde{\mathbf{m}}\,|q_1]$ is the probability to observe the time reverse trajectory $\tilde{\mathbf{m}}$ in the backward process given the initial state q_1 of the time reverse trajectory. Equations (4) and (3) together imply (2).

Equation (2) can be rewritten as follows:

$$\mathcal{P}_{\rm F}[\mathbf{m}] = \mathcal{P}_{\rm B}[\tilde{\mathbf{m}}] \exp\left(\frac{\Delta S_{\rm tot}[\mathbf{m}]}{k_{\rm B}}\right). \tag{5}$$

For the time reverse process, let us *define*:

$$\Delta \tilde{S}_{\rm tot}[\tilde{\mathbf{m}}] = k_{\rm B} \log \frac{\mathcal{P}_{\rm B}[\tilde{\mathbf{m}}]}{\mathcal{P}_{\rm F}[\mathbf{m}]} = -\Delta S_{\rm tot}[\mathbf{m}]. \tag{6}$$

With this definition, integrating (5) over all the trajectories that produce the same amount of entropy $\Delta S_{\rm tot}$, we recover (1) with [13, 14]:

$$P(\Delta S_{\rm tot}) = \int \mathcal{P}_{\rm F}[\mathbf{m}]\ \delta\left(\Delta S_{\rm tot}[\mathbf{m}] - \Delta S_{\rm tot}\right) {\rm d}\mathbf{m}, \tag{7}$$

$$\tilde{P}(\Delta S_{\rm tot}) = \int \mathcal{P}_{\rm B}[\tilde{\mathbf{m}}]\ \delta\left(\Delta \tilde{S}_{\rm tot}[\tilde{\mathbf{m}}] - \Delta S_{\rm tot}\right) {\rm d}\tilde{\mathbf{m}}. \tag{8}$$

However, $\Delta \tilde{S}_{\rm tot}[\tilde{\mathbf{m}}]$ defined in equation (6) *is not the amount of entropy produced by the trajectory in the time reverse process*. The latter is equal to

$$\Delta S^{\rm B}_{\rm tot}[\tilde{\mathbf{m}}] = \frac{Q_{\rm B}[\tilde{\mathbf{m}}]}{T} + \Delta S_{\rm B}[\tilde{\mathbf{m}}], \tag{9}$$

where $Q_{\rm B}[\tilde{\mathbf{m}}]$ is the amount of heat dissipated to the environment in the time reverse process along the trajectory $\tilde{\mathbf{m}}$ and $\Delta S_{\rm B}[\tilde{\mathbf{m}}]$ is the variation of the entropy of the system. The heat released to the environment is odd under time reversal:

$$Q_{\rm B}[\tilde{\mathbf{m}}] = k_{\rm B} \log \frac{\mathcal{P}_{\rm B}\left[\tilde{\mathbf{m}}\,\middle|q_1\right]}{\mathcal{P}_{\rm F}\left[\mathbf{m}\,\middle|q_0\right]} = -Q[\mathbf{m}]. \tag{10}$$

However, this is not the case for the variation of the entropy of the system:

$$\Delta S_{\rm B}[\tilde{\mathbf{m}}] = -k_{\rm B} \log \frac{\rho_2(q_0)}{\rho_1(q_1)} \neq -\Delta S[\mathbf{m}] = k_{\rm B} \log \frac{\rho_0(q_0)}{\rho_1(q_1)}. \tag{11}$$

Therefore, $\Delta S^{\rm B}_{\rm tot}[\tilde{\mathbf{m}}] \neq -\Delta S_{\rm tot}[\mathbf{m}] = \Delta \tilde{S}_{\rm tot}[\tilde{\mathbf{m}}]$, and the quantity defined in (6) and entering the fluctuation theorem is not the amount of entropy produced by the trajectory $\tilde{\mathbf{m}}$ in the backward process.

[7] We assume here that the system does not have degrees of freedom that are odd under time reversal such as velocities. The variables odd under time reversal should have their sign changed in $\tilde{\mathbf{m}}$.

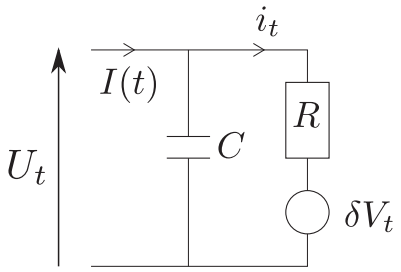

Figure 2. Sketch of the experimental setup. A resistor of $R = 1$ MΩ is connected in parallel with a capacitor of $C = 1$ nF. The voltage source δV_t in series with the resistor represents Johnson–Nyquist noise.

The expression of the entropy $\Delta S^{\mathrm{B}}_{\mathrm{tot}}[\tilde{\mathbf{m}}]$ produced in the backward process in terms of probability of paths is:

$$\Delta S^{\mathrm{B}}_{\mathrm{tot}}[\tilde{\mathbf{m}}] = k_{\mathrm{B}} \log \frac{\mathcal{P}_{\mathrm{B}}\left[\tilde{\mathbf{m}} \,\middle|\, q_1\right]\rho_1(q_1)}{\mathcal{P}_{\mathrm{F}}\left[\mathbf{m} \,\middle|\, q_0\right]\rho_2(q_0)}. \tag{12}$$

In fact, while $\mathcal{P}_{\mathrm{B}}[\tilde{\mathbf{m}}\,|q_1]\rho_1(q_1) = \mathcal{P}_{\mathrm{B}}[\tilde{\mathbf{m}}]$ is the probability to observe the trajectory $\tilde{\mathbf{m}}$ in the backward process, the probability to observe the trajectory $\mathbf{m}$ in the *time-reversal of the backward process* is $\mathcal{P}_{\mathrm{F}}[\mathbf{m}\,|q_0]\rho_2(q_0)$. In general, it is different from the probability to observe the trajectory $\mathbf{m}$ in the forward process: $\mathcal{P}_{\mathrm{F}}[\mathbf{m}\,|q_0]\rho_2(q_0) \neq \mathcal{P}_{\mathrm{F}}[\mathbf{m}] = \mathcal{P}_{\mathrm{F}}[\mathbf{m}\,|q_0]\rho_0(q_0)$ because in general the final macroscopic state of the backward process is not equal to the initial macroscopic state of the forward process, $\rho_2(q_0) \neq \rho_0(q_0)$.

We call $\Delta\tilde{S}_{\mathrm{tot}}[\tilde{\mathbf{m}}]$ the *conjugated entropy production*. Using its definition (6) and the expression for the heat dissipated in the backward process (10), we obtain that:

$$\Delta\tilde{S}_{\mathrm{tot}}[\tilde{\mathbf{m}}] = \frac{Q_{\mathrm{B}}[\tilde{\mathbf{m}}]}{T} + \Delta\tilde{S}[\tilde{\mathbf{m}}], \tag{13}$$

where

$$\Delta\tilde{S}[\tilde{\mathbf{m}}] = -k_{\mathrm{B}} \log \frac{\rho_0(q_0)}{\rho_1(q_1)} = -\Delta S[\mathbf{m}]. \tag{14}$$

Equations (13) and (14) allow one to do a physical interpretation of the conjugated entropy production. The conjugated entropy production is equal to the variation of the entropy of the environment in the backward process minus the variation of the entropy of the system in the forward process.

The conjugated entropy production is equal to the entropy produced in the backward process, $\Delta\tilde{S}_{\mathrm{tot}}[\tilde{\mathbf{m}}] = \Delta S^{\mathrm{B}}_{\mathrm{tot}}[\tilde{\mathbf{m}}]$, if and only if $\rho_0(q_0) = \rho_2(q_0)$, i.e. if the final macroscopic state of the backward process is also the initial state of the forward process. This is the case in the transition between equilibrium states and in non-equilibrium stationary states. However, in the transition between two arbitrary non-equilibrium, non-stationary states, it has no reason to be fulfilled.

The difference between $\Delta\tilde{S}_{\mathrm{tot}}[\tilde{\mathbf{m}}]$ and $\Delta S^{\mathrm{B}}_{\mathrm{tot}}[\tilde{\mathbf{m}}]$ is:

$$\Delta\tilde{S}_{\mathrm{tot}}[\tilde{\mathbf{m}}] - \Delta S^{\mathrm{B}}_{\mathrm{tot}}[\tilde{\mathbf{m}}] = \Delta\tilde{S}[\tilde{\mathbf{m}}] - \Delta S_{\mathrm{B}}[\tilde{\mathbf{m}}] = k_{\mathrm{B}} \log \frac{\rho_2(q_0)}{\rho_0(q_0)}. \tag{15}$$

When averaging over many trajectories of the backward process, this difference is positive:

$$\langle\Delta\tilde{S}_{\mathrm{tot}}\rangle - \langle\Delta S^{\mathrm{B}}_{\mathrm{tot}}\rangle = k_{\mathrm{B}} \int \rho_2(q_0) \log \frac{\rho_2(q_0)}{\rho_0(q_0)} \mathrm{d}q_0 \geqslant 0. \tag{16}$$

The right-hand side of (16) is the *relative entropy* or *Kullback–Leibler divergence* between the distributions ρ_2 and ρ_0. This quantity is non-negative and it is zero if and only the two distributions ρ_2 and ρ_0 are indistinguishable [38].

3. Experimental setup

3.1. The system

The experimental setup is sketched in figure 2. A resistor of resistance $R = 1$ MΩ is connected in parallel with a condenser of capacity $C = 1$ nF. The input current $I(t)$ is oscillating at a frequency of f_{d}, $I(t) = I_{\max} \sin(\omega t)$ with $\omega = 2\pi f_{\mathrm{d}}$. The time constant of the circuit is $\tau_{\mathrm{c}} = RC \approx 1$ ms.

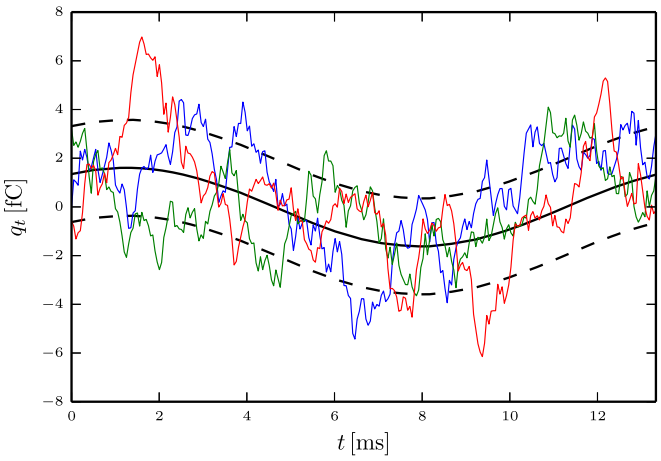

Figure 3. Three examples of stochastic trajectories during one period of the driving signal (red, green and blue strongly fluctuating lines). The black solid line represents the ensemble average $\langle q_t \rangle$ and the black dashed lines represent the ensemble average plus and minus one standard deviation $\sigma_t = \sqrt{\left\langle (q_t - \langle q_t \rangle)^2 \right\rangle}$. In this example, the driving frequency is $f_d = 75$ Hz and the amplitude of the driving is $q^*_{max} = 2.3$ fC. The average and standard deviation are estimated from 38 164 trajectories.

The voltage across the resistor fluctuates due to Johnson–Nyquist noise, which is modeled in figure 2 by putting a voltage source in series with the resistor. At any time, this source produces a random voltage δV_t satisfying [39, 40]:

$$\langle \delta V_t \rangle = 0, \tag{17}$$

$$\langle \delta V_t \delta V_{t'} \rangle = 2k_B\, TR\, \delta(t - t'). \tag{18}$$

We denote q_t the charge that has flown through the resistor at time t and $i_t = \mathrm{d}q_t/\mathrm{d}t$ is the current that flows through it. Moreover, let $q^*{}_t = \int_{-\infty}^{t} I(s)\,\mathrm{d}s$ the total charge that has flown through the circuit at time t. The charge of the capacitor is thus $q_t^* - q_t$ and the voltage across the circuit is equal to:

$$U_t = \frac{q_t^* - q_t}{C}. \tag{19}$$

Ohm's law for the resistor implies that:

$$U_t = Ri_t + \delta V_t. \tag{20}$$

Hence, the charge q_t obeys the following Langevin equation:

$$R\frac{\mathrm{d}q_t}{\mathrm{d}t} = -\frac{1}{C}\left(q_t - q_t^*\right) + \delta V_t. \tag{21}$$

This equation is identical to the equation of motion of an overdamped Brownian particle whose position is q_t, its friction coefficient is R and is trapped with a harmonic trap of stiffness $1/C$ centered at q_t^*. Our control parameter is q_t^*. It oscillates sinusoidally at frequency f_d and its amplitude is related to the amplitude of the input current through $q^*_{max} = I_{max}/\omega$. In figure 3, we plot three examples of realizations of the stochastic trajectory q_t, together with the ensemble average.

3.2. Protocol

After a transient that we do not analyze here, the system relaxes toward a time periodic stationary state. In other words, the probability distribution $\rho(q, t)$ of the charge q at time t is time periodic of period $1/f_d$, the period of the driving signal. We use this periodicity of $\rho(q, t)$ to construct an ensemble of non-equilibrium trajectories.

Here is how we construct the ensembles of forward and backward trajectories of duration τ from a long quasistationary trajectory $\{q_t\}$. We chose the origin of time such that $q_t^* = q^*_{max} \cos(\omega t)$, where $\omega = 2\pi f_d$. Let $\tau_d \geqslant \tau$ be an integer multiple of the driving period $1/f_d$. The nth member of the forward ensemble is the portion of $\{q_t\}$ where $(2n+1)\tau_d - \tau \leqslant t \leqslant (2n+1)\tau_d$, n being an integer. The corresponding member of the backward ensemble is the portion of $\{q_t\}$ where $(2n+1)\tau_d \leqslant t \leqslant (2n+1)\tau_d + \tau$.

On figure 4, we sketch how the first two members of the forward and backward ensembles are obtained for $\tau_d = 1/f_d$. The blue portions correspond to members of the forward ensemble and the green portions to

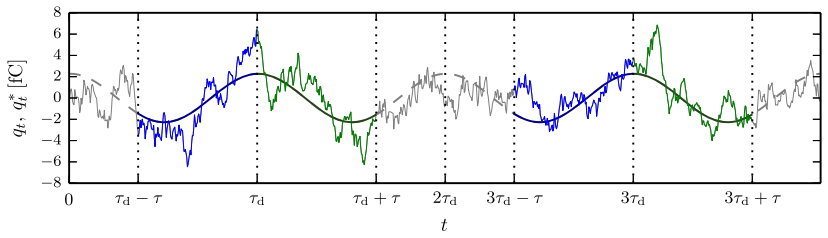

Figure 4. Construction of the ensemble of non-equilibrium trajectories for a process duration of $\tau = 8.4$ ms from a long stationary trajectory driven at $f_d = 75$ Hz. Since $\tau < 1/f_d = 13.3$ ms, we set $\tau_d = 1/f_d$. The smoothly oscillating thick curve represents the control parameter q_t^*. The strongly fluctuating thin curve represents q_t. The blue portions correspond to members of the forward ensemble and the green portions to members of the backward ensemble. The forward trajectories start at time $(2n+1)\tau_d - \tau$ and end at time $(2n+1)\tau_d$, and the backward trajectories start at time $(2n+1)\tau_d$ and end at time $(2n+1)\tau_d - \tau$, where n is an integer (here, we plot $n = 0$ and $n = 1$). Due to the periodicity of the driving protocol, each member of the forward ensemble is subject to the same driving signal and due to the symmetry of the driving signal, the protocol in each backward process is the time reverse of the protocol in the forward process.

members of the backward ensemble. The smoothly oscillating curve represents the driving signal q_t^* and the strongly fluctuating curve is q_t.

Due to the periodicity of the driving protocol, all the members of the forward ensemble are subjected to the same driving signal. Moreover, since $\rho(q, t)$ is time periodic of period τ_d, all the initial mesoscopic states of the forward trajectories are drawn from the same initial distribution $\rho_0(q)$ and hence all the forward trajectories are drawn from the same path distribution $\mathcal{P}_F$. The same reasoning applies the backward trajectories: their initial mesoscopic state is drawn from the same distribution $\rho_1(q)$ and they are all submitted to the same driving. Hence they are all drawn from the same path distribution $\mathcal{P}_B$. Finally, the origin of time was chosen such that q_t^* is symmetric around $n\tau_d$, $q^*_{n\tau_d - t} = q^*_{n\tau_d + t}$. Hence the members of the backward ensemble are subjected to a driving that is the time reversal of the driving under which the members of the forward ensemble are submitted.

3.3. Measurement of stochastic entropy production

The amount of entropy produced along a stochastic trajectory $\mathbf{m}$ is calculated using (3): $\Delta S_{tot}[\mathbf{m}] = Q[\mathbf{m}]/T + \Delta S[\mathbf{m}]$. Following Sekimoto [17], the heat released to the environment in the time interval $[t, t + dt]$ is given by

$$dQ_t = \left(R\frac{dq_t}{dt} + \delta V_t\right) \circ dq_t = -\frac{1}{C}\left(q_t - q_t^\star\right) \circ dq_t, \tag{22}$$

where $\circ$ denotes Stratonovich product and the second equality is consequence of (21). Note that the amount of heat released per unit time is the sum of two contributions, $\dot{Q}_t = \dot{Q}_t^{\text{Joule}} + \dot{Q}_t^{\text{thermal}}$. The first contribution is due to the Joule heating inside the resistor: $\dot{Q}_t^{\text{Joule}} = Ri_t^2$, and the second to the power injected by thermal fluctuations: $\dot{Q}_t^{\text{thermal}} = \delta V_t i_t$. The heat dissipated between times t_0 and t_1 along a stochastic trajectory $\mathbf{m}$ equals to

$$Q[\mathbf{m}] = \int_{t_0}^{t_1} dQ_t = -\int_{t_0}^{t_1} \frac{q_t - q_t^*}{C} \circ dq_t, \tag{23}$$

which is measured from the stochastic trajectories.

The trajectory dependent entropy is given by $S(q_t, t) = -k_B \log \rho(q_t, t)$, where $\rho(q_t, t)$ is the probability distribution of the charge q_t at time t. The distribution $\rho(q_t, t)$ is estimated from the ensemble of trajectories. The system's entropy change along a trajectory $\mathbf{m}$ that starts at q_0 at time t_0 and ends at q_1 at time t_1 is obtained as

$$\Delta S[\mathbf{m}] = S\left(q_1, t_1\right) - S\left(q_0, t_0\right) = -k_B \log \rho\left(q_1, t_1\right) + k_B \log \rho\left(q_0, t_0\right). \tag{24}$$

4. Experimental results

Figures 5 and 6 summarize the thermodynamics of the process as a function of the process duration τ for a driving frequency of $f_d = 75$ Hz, and hence a driving period of $1/f_d \approx 13.3$ ms, and a driving amplitude of $q^*_{max} = 2.3$ fC. We consider durations up to one period of the driving signal and hence we set $\tau_d = 1/f_d$. The signal q_t was sampled at 20 kHz and the ensemble consists of 38 164 trajectories.

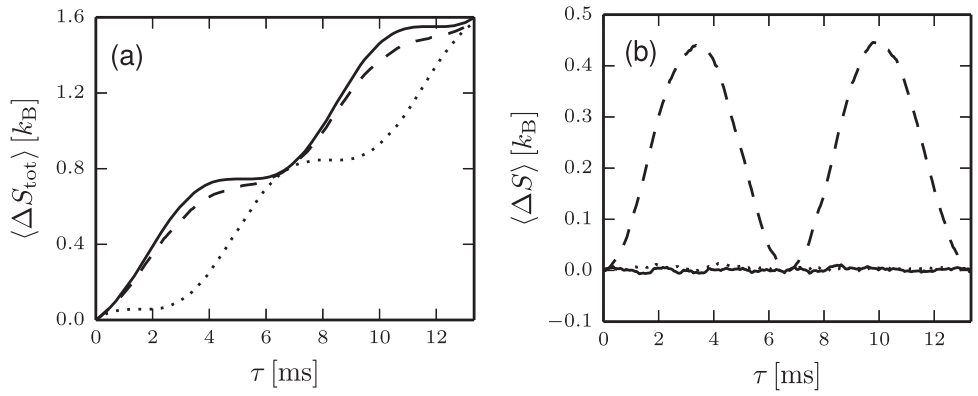

Figure 5. (a) Average entropy production as a function of the process duration τ. The solid line represents the entropy production in the forward process, the dotted line the entropy production in the backward process and the dashed line the conjugated entropy production $\Delta\tilde{S}_{\rm tot}[\tilde{\mathbf{m}}]$. (b) Average variation of the entropy $\Delta S\,[\mathbf{m}]$ of the system in the forward (solid line) and in the time reverse process (dotted line). They are both equal to zero for all τ. The dashed line represents the average of $\Delta\tilde{S}[\tilde{\mathbf{m}}]$ over the time reverse process.

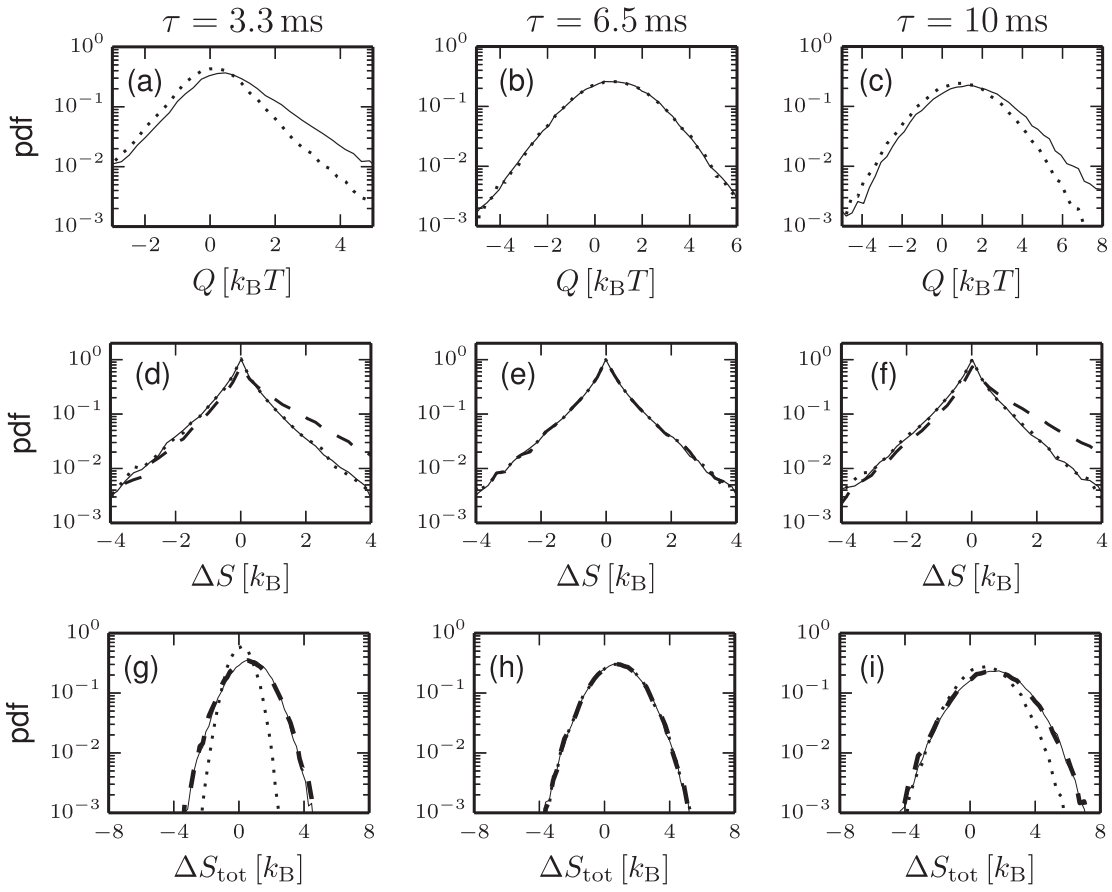

Figure 6. Distributions of the heat (top), system entropy variation (middle) and entropy production (bottom) for the three different durations $\tau \approx 3.3$, 6.5 and 10 ms corresponding respectively to one quarter, one half and three quarters of the driving period $\tau_{\rm d}$. Each column corresponds to one value of τ. Upper row (panels (a), (b), and (c)): distributions of the heat dissipated in the forward (solid lines) and time reverse process (dashed lines). Middle row (panels (d), (e), and (f)): distributions of the variation of the entropy of the system in the forward process (solid lines), in the time reverse process (dotted lines) and of $\Delta\tilde{S}[\tilde{\mathbf{m}}]$ given by (14) in the time reverse process (dashed lines). Lower row (panels (g), (h), and (i)): Distribution $P\,(\Delta S_{\rm tot})$ of the entropy produced in the forward process (solid lines), distribution $P_{\rm B}\,(\Delta S_{\rm tot})$ of the entropy produced in the backward process (dotted lines), and distribution $\tilde{P}(\Delta S_{\rm tot})$ of the conjugated entropy production (dashed lines).

Figure 5(a) shows the ensemble averages of the amount of entropy produced in the forward process, $\langle \Delta S_{\rm tot} \rangle$ (solid line), the amount of entropy produced in the backward process $\langle \Delta S^{\rm B}_{\rm tot} \rangle$ (dotted line) and of the conjugated entropy production $\langle \Delta\tilde{S}_{\rm tot} \rangle$ (dashed line) as a function of the process duration τ. These three quantities increase

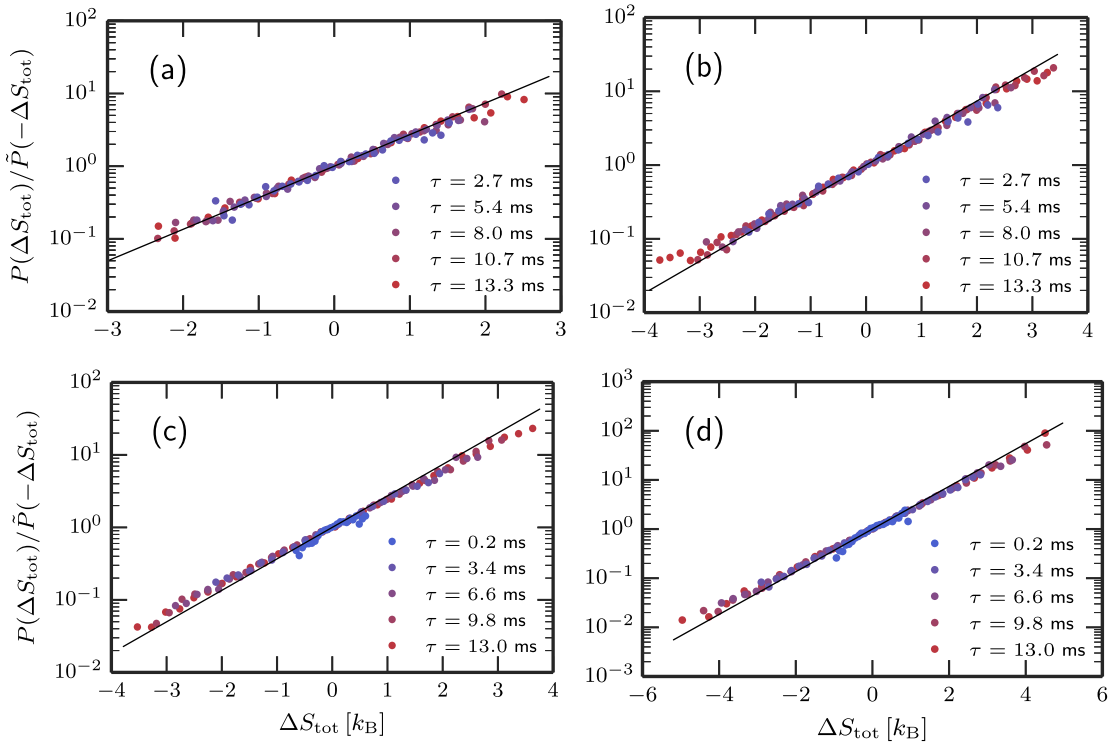

Figure 7. Ratio $P(\Delta S_{\rm tot})/\tilde{P}(-\Delta S_{\rm tot})$ on a logarithmic scale as a function of $\Delta S_{\rm tot}$ for different driving frequencies, amplitudes and durations τ. The black line corresponds to the theoretical prediction $\exp(\Delta S_{\rm tot}/k_{\rm B})$. Panel (a): driving frequency $f_{\rm d} = 75$ Hz, period $1/f_{\rm d} = 13.3$ ms, amplitude $q^*_{\rm max} = 1.4$ fC. Panel (b): driving frequency $f_{\rm d} = 75$ Hz, period $1/f_{\rm d} = 13.3$ ms, amplitude $q^*_{\rm max} = 2.3$ fC. Panel (c): driving frequency $f_{\rm d} = 1$ kHz, period $1/f_{\rm d} = 1$ ms $\approx RC$, amplitude $q^*_{\rm max} = 0.86$ fC. Panel (d): driving frequency $f_{\rm d} = 1$ kHz, period $1/f_{\rm d} = 1$ ms $\approx RC$, amplitude $q^*_{\rm max} = 1.3$ fC. For panels (c) and (d), we considered durations up to 13 driving periods, hence $\tau_{\rm d} = 13$ ms.

with τ, in a manner that is roughly linear with a periodic modulation. We check the inequality (16), $\langle \Delta \tilde{S}_{\rm tot} \rangle \geqslant \langle \Delta S^{\rm B}_{\rm tot} \rangle$. Moreover, the average amount of entropy produced in the forward process is approximately equal to the average conjugated entropy production, $\langle \Delta S_{\rm tot} \rangle \approx \langle \Delta \tilde{S}_{\rm tot} \rangle$.

We also investigate the average value of the system's entropy change (figure 5(b)) in the forward process, $\langle \Delta S \rangle$ (solid line), in the time reverse $\langle \Delta S_{\rm B} \rangle$ (dotted line) and the quantity $\langle \Delta \tilde{S} \rangle$ (dashed line) as a function of the process duration τ. The system's entropy change vanishes on average both in forward and backward processes. Hence, the average entropy production is equal to the average dissipated heat in both cases, $\langle \Delta S_{\rm tot} \rangle = \langle Q \rangle / T$ and $\langle \Delta S^{\rm B}_{\rm tot} \rangle = \langle Q_{\rm B} \rangle / T$.

In this situation (15) and (16) imply

$$\langle \Delta \tilde{S}_{\rm tot} \rangle - \langle \Delta S^{\rm B}_{\rm tot} \rangle = \langle \Delta \tilde{S} \rangle = k_{\rm B} \int \rho_2(q) \log \frac{\rho_2(q)}{\rho_0(q)} \, {\rm d}q \geqslant 0. \tag{25}$$

On figure 5(b) we can see that $\langle \Delta \tilde{S} \rangle$ is non-negative for all τ, in accordance with (25). The quantity $\langle \Delta \tilde{S} \rangle$ is zero for $\tau = 0$, $\tau = \tau_{\rm d}/2 \approx 6.5$ ms and $\tau = \tau_{\rm d}$, implying that for these durations, $\rho_2 \equiv \rho_0$. In fact, for $\tau = 0$, we have $t_0 = t_1 = t_2$ and there is no process and hence $\rho_0 \equiv \rho_1 \equiv \rho_2$. For $\tau = \tau_{\rm d}/2$, we have $t_2 - t_0 = \tau_{\rm d}$, and hence $\rho_2(q) = \rho(q, t_0 + \tau_{\rm d}) = \rho(q, t_0) = \rho_0(q)$ because $\rho(q, t)$ is time periodic with period $\tau_{\rm d}$. The same reasoning applies for $\tau = \tau_{\rm d}$. In that case, we have $t_2 - t_0 = 2\tau_{\rm d}$, and hence $\rho_2(q) = \rho(q, t_0 + 2\tau_{\rm d}) = \rho(q, t_0) = \rho_0(q)$. The quantity $\langle \Delta \tilde{S} \rangle$ is also zero for $\tau = \tau_{\rm d}/2 \approx 6.5$ ms which is one half of the driving period. Finally, $\langle \Delta \tilde{S} \rangle$ is maximum for $\tau \approx 3.3$ ms and $\tau \approx 10$ ms which correspond to one fourth and three fourth of the driving period.

On figure 6, we show the distributions of the thermodynamic quantities heat, entropy variation and entropy production in the forward and backward process for the three durations $\tau \approx 3.3, 6.5$ and 10 ms, corresponding to one quarter, one half and three quarters of the period of the driving signal.

The first row of figure 6 (panels (a), (b), and (c)) shows the distributions of the heat released to the environment in the forward (solid lines) and in the time reverse process (dashed lines). These are identical for $\tau \approx 6.5$ ms otherwise they are different.

In the middle row (panels (d), (e) and (f)), we show the distributions of the system's entropy change in the forward process (solid lines) in the backward process (dotted lines) and of the quantity $\Delta\tilde{S}$ (dashed lines). The distributions of the system's entropy change in forward and backward processes are identical. They are symmetric with respect to 0 and non-Gaussian for all values of τ. Similar results were also found in [27, 32]. The distribution of $\Delta\tilde{S}[\tilde{\mathbf{m}}]$ differs from the two others except for $\tau \approx 6.5$ ms.

The lower row (panels (g), (h) and (i)) of figure 6 shows the distribution $P(\Delta S_{\rm tot})$ of the entropy produced in the forward process (solid lines), the distribution $P_{\rm B}(\Delta S_{\rm tot})$ of the entropy produced in the backward process (dotted lines) and the distribution $\tilde{P}(\Delta S_{\rm tot})$ of the conjugated entropy production (dashed lines). The three distributions are Gaussian, as in [27]. The distributions of the entropy produced in the forward process and of the conjugated entropy production are equal, $P(\Delta S_{\rm tot}) = \tilde{P}(\Delta S_{\rm tot})$. The distribution $P_{\rm B}(\Delta S_{\rm tot})$ of the entropy produced in the backward process is equal to the two others for $\tau = 6.5$ ms, otherwise it has a different shape. In accordance with equation (16) and with figure 5(a), its mean is smaller than the mean of the two others. Moreover, its variance is also smaller. Note that a necessary condition for the fluctuation theorem (1) to hold when the distributions $P(\Delta S_{\rm tot})$ and $\tilde{P}(\Delta S_{\rm tot})$ are Gaussian is that they are equal [24, 41].

Figure 7 shows that the theorem (1) is verified with high accuracy in our experiment. This figure shows the ratio $P(\Delta S_{\rm tot})/\tilde{P}(-\Delta S_{\rm tot})$ between the distribution $P(\Delta S_{\rm tot})$ of the entropy produced in the forward process and of the distribution $\tilde{P}(-\Delta S_{\rm tot})$ of (minus) the conjugated entropy production $-\Delta\tilde{S}_{\rm tot}[\tilde{\mathbf{m}}]$ for the backward process for different driving frequencies and amplitudes and for the durations. Panels (a) and (b) correspond to a driving frequency of $f_{\rm d} = 75$ Hz and hence a driving period of $1/f_{\rm d} = 13.3$ ms. The signal q_t was sampled at 20 kHz. The driving amplitudes are $q^{\star}_{\rm max} = 1.4$ fC for panel (a) and $q^{\star}_{\rm max} = 2.3$ fC for panel (b). The ensembles consist of 38 424 (panel (a)) and 38 164 (panel (b)) trajectories. Panels (c) and (d) correspond to a driving frequency of $f_{\rm d} = 1$ kHz and hence the driving period is $1/f_{\rm d} = 1$ ms $\approx RC$, which is the time constant of the circuit. Here, we considered process durations up to 13 periods, and hence $\tau_{\rm d} = 13/f_{\rm d} = 13$ ms. The signal q_t was sampled at 100 kHz and the ensembles consist of 198 144 trajectories. The driving amplitudes are $q^{\star}_{\rm max} = 0.86$ fC for panel (c) and $q^{\star}_{\rm max} = 1.3$ fC for panel (d). The black solid line corresponds to the theory, $\exp(\Delta S_{\rm tot}/k_{\rm B})$. The fluctuation theorem (1) is fulfilled with high accuracy (along up to four decades) for all the durations considered.

5. Conclusion

To summarize, in this work we have studied experimentally the thermodynamics of the transition between two non-equilibrium states in a parallel *RC* circuit, in the light of the fluctuation theorem for the entropy production (1). In such a situation, the fluctuation theorem (1) presents a subtlety: for the backward process it involves the distribution of the *conjugated entropy production* (6) rather than the distribution of the entropy production.

We have characterized the statistics of the heat dissipation, entropy variation and entropy production in the forward and backward processes. In particular, for the backward process, we have studied the difference between entropy production and conjugated entropy production. Furthermore, we have verified that the detailed fluctuation theorem is fulfilled with high accuracy for different driving frequencies and amplitudes and for different process durations, which confirms the universality of the result.

Acknowledgments

LG acknowledges the Max-Planck-Institut für Physik komplexer Systeme for its hospitality. LG and ÉR acknowledge financial support from Grant ENFASIS (FIS2011-22644) and TerMic (FIS2014-52486-R) from the Spanish Government. SC also acknowledges financial support from ERC project OUTEFLUCOP.

References

[1] Szilard L 1925 *Z. Phys.* **32** 753–88
[2] Wang G M, Sevick E M, Mittag E, Searles D J and Evans D J 2002 *Phys. Rev. Lett.* **89** 050601
[3] Collin D, Ritort F, Jarzynski C, Smith S B, Tinoco I and Bustamante C 2005 *Nature* **437** 231–4
[4] Evans D J, Cohen E G D and Morriss G P 1993 *Phys. Rev. Lett.* **71** 2401–4
[5] Gallavotti G and Cohen E G D 1995 *Phys. Rev. Lett.* **74** 2694–7
[6] Jarzynski C 1997 *Phys. Rev. Lett.* **78** 2690–3
[7] Crooks G E 1998 *J. Stat. Phys.* **90** 1481–7
[8] Crooks G E 1999 *Phys. Rev.* E **60** 2721–6
[9] Hatano T and Sasa S I 2001 *Phys. Rev. Lett.* **86** 3463–6
[10] Seifert U 2005 *Phys. Rev. Lett.* **95** 040602
[11] Harris R J and Schütz G M 2007 *J. Stat. Mech.* **2007** P07020
[12] Saha A, Lahiri S and Jayannavar A M 2009 *Phys. Rev.* E **80** 011117

[13] Esposito M and Van den Broeck C 2010 *Phys. Rev. Lett.* **104** 090601
[14] Spinney R E and Ford I J 2012 Fluctuation relations: a pedagogical overview *Nonequilibrium Statistical Physics of Small Systems: Fluctuation Relations and Beyond* (Weinheim: Wiley)
[15] Sekimoto K 1998 *Prog. Theor. Phys. Suppl.* **130** 17–27
[16] Esposito M and d Broeck C V 2011 *Europhys. Lett.* **95** 40004
[17] Sekimoto K 2012 *Stochastic Energetics* 2010 edn (Berlin: Springer)
[18] Seifert U 2012 *Rep. Prog. Phys.* **75** 126001
[19] Deffner S and Lutz E 2012 arXiv:1201.3888
[20] Granger L 2013 Irreversibility and information *PhD Thesis* Technische Universität Dresden Dresden, Germany
[21] Roldan E 2014 *Irreversibility and Dissipation in Microscopic Systems* (Berlin: Springer)
[22] Liphardt J, Dumont S, Smith S B, Tinoco I and Bustamante C 2002 *Science* **296** 1832–5
[23] Trepagnier E H, Jarzynski C, Ritort F, Crooks G E, Bustamante C J and Liphardt J 2004 *Proc. Natl Acad. Sci. USA* **101** 15038–41
[24] Douarche F, Ciliberto S and Petrosyan A 2005 *J. Stat. Mech.* **2005** P09011
[25] Tietz C, Schuler S, Speck T, Seifert U and Wrachtrup J 2006 *Phys. Rev. Lett.* **97** 050602
[26] Andrieux D, Gaspard P, Ciliberto S, Garnier N, Joubaud S and Petrosyan A 2007 *Phys. Rev. Lett.* **98** 150601
[27] Joubaud S, Garnier N B and Ciliberto S 2008 *Europhys. Lett.* **82** 30007
[28] Mestres P, Martinez I A, Ortiz-Ambriz A, Rica R A and Roldan E 2014 *Phys. Rev.* E **90** 032116
[29] Koski J V, Sagawa T, Saira O P, Yoon Y, Kutvonen A, Solinas P, Möttönen M, Ala-Nissila T and Pekola J P 2013 *Nat. Phys.* **9** 644–8
[30] Thingna J, Hänggi P, Fazio R and Campisi M 2014 *Phys. Rev.* B **90** 094517
[31] Bonança M V S and Deffner S 2014 *J. Chem. Phys.* **140** 244119
[32] Martínez I A, Roldán É, Dinis L, Petrov D and Rica R A 2015 *Phys. Rev. Lett.* **114** 120601
[33] Ritort F, Bustamante C and Tinoco I 2002 *Proc. Natl Acad. Sci.* **99** 13544–8
[34] Kawai R, Parrondo J M R and den Broeck C V 2007 *Phys. Rev. Lett.* **98** 080602
[35] Gomez-Marin A, Parrondo J M R and Broeck C V d 2008 *Europhys. Lett.* **82** 50002
[36] Parrondo J M R, Broeck C V D and Kawai R 2009 *New J. Phys.* **11** 073008
[37] Kurchan J 1998 *J. Phys. A: Math. Gen.* **31** 3719
[38] Cover T M and Thomas J A 1991 *Elements of Information Theory* 99th edn (New York: Wiley)
[39] van Zon R, Ciliberto S and Cohen E G D 2004 *Phys. Rev. Lett.* **92** 130601
[40] Garnier N and Ciliberto S 2005 *Phys. Rev.* E **71** 060101
[41] Granger L, Niemann M and Kantz H 2010 *J. Stat. Mech.* **2010** P06029